FEM-DEM Simulation of Two-way Fluid-Solid Interaction in Fibrous Porous Media

K. Yazdchi, S. Srivastava and S. Luding

Multi Scale Mechanics (MSM), MESA+ Institute for Nanotechnology, Faculty of Engineering Technology, University of Twente, P.O. Box 217, 7500 AE Enschede, The Netherlands

Abstract. Fluid flow through particulate media is pivotal in many industrial processes, e.g. in fluidized beds, granular storage, industrial filtration and medical aerosols. Flow in these types of media is inherently complex and challenging to simulate, especially when the particulate phase is mobile. The goals of this paper are twofold: (i) the derivation of accurate correlations for the drag force, taking into account the effect of microstructure, to improve the higher scale macro-models and (ii) incorporating such closures into a "compatible" monolithic multi-phase/scale model that uses a (particle-based) Delaunay triangulation (DT) of space as basis – in future, possibly, involving also multiple fields.

INTRODUCTION

The modeling of realistic systems is already a challenge when several fields are involved only on a single scale. Usually fields or phases, e.g. discrete particles, solid walls and fluids/gases, are coupled and affect each other continuously at different length scales. Examples are fluidized bed reactors in chemical engineering, mechanical engineering unit-processes like silos, mixers, ball-mills, or conveyor belts, modern engineering materials like composite materials, or geotechnical/physical systems [1-5].

The particle (solid) phase is usually described by means of the so-called discrete element method (DEM), where all information on particle position, velocity and forces is available in detail [6]. DEM is essentially a numerical technique to model the motion of an assembly of particles interacting with each other through contact forces. It is quite efficient for investigating phenomena occurring at the length scale of a particle diameter and larger. On the other hand, continuum methods are used for chemical engineering applications like granular and gas-particle flows [7] silos with unusual flow-zones and geometries [8], fluid flow, aerodynamics, and many others, on much smaller or much larger scales. Attempts to couple distinct particle- and continuum methods have been successful [9] but are still subject of ongoing research.

The prime difficulty of modeling two-phase gas/fluid-solid flows is the interphase coupling, which accounts for the effects of gas/fluid flow on the solids motion and vice versa. Among all the coupling terms emerging from averaging (e.g. fluid-particle drag, added-mass, lift, history, Magnus forces, and particle and fluid phase stresses), the fluid-particle drag is the primary force affecting, suspending and moving the particles, with considerable influence on, e.g. the bed expansion and stability of a suspension. The drag force depends (among many parameters such as particle size/spatial distribution, particle shape, and orientation, etc.) on the local relative velocity between phases and the average/effective local porosity [4]. It was shown in several case studies that the drag law can have a significant influence on both qualitative and quantitative nature of the flow [10]. Therefore, establishing accurate drag force relations is crucial for obtaining good models and has challenged both physics and engineering community for many years.

This paper features a reformulated drag force model for monodisperse fiber arrays as function of microstructural parameters that improve the consistency, accuracy and computational efficiency compared to those available until now, since it is valid for all porosities. Furthermore, a coarse-grained finite element (FE) framework based on coupling an unstructured FE mesh and a soft-sphere DEM for moving particles is proposed. The fluid-particle interactions are incorporated using the above drag closures. This approach allows computing the dynamics of particles and fluid using a deforming mesh, while resolving the fluid/gas flow around the particles on the same scale.

DRAG FORCE MODEL

The drag force accounts for the resistance to the flow through a porous media, and is inversely related to its permeability, K. The permeability is the proportionality constant in Darcy's equation

$$\vec{U} = \frac{-K\nabla p}{\mu}, \qquad (1)$$

where $\nabla p, \mu$ and U are pressure gradient, viscosity and superficial fluid velocity, respectively. The superficial velocity is defined as

$$\vec{U} = \frac{1}{V}\int_{V_f} \vec{u}\, dV = \varepsilon\langle\vec{u}\rangle, \qquad (2)$$

where V, V_f and $\varepsilon = V_f/V$ are total available volume, the volume of fluid and porosity, respectively. Following Yazdchi et al. [2], the permeability, K is related to the drag coefficient, β as

$$\beta = \frac{\mu\varepsilon^2}{d^2\lambda}, \qquad (3)$$

where $\lambda = K/d^2$ represents the non-dimensional permeability and is often used instead of K in literature. Ergun's equation is a commonly used drag law, which is a non-linear function of porosity, fluid velocity and particle size. It accurately predicts the total drag force for a limited range of porosities in 3D. An aptly modified version of this equation applicable in 2D is deployed as suggested in [11]. By employing fully resolved FE simulations of flows through static, regular and random arrays of cylinders, Yazdchi et al. [3] showed that the mean values of the 2nd nearest neighbor distances of fibres, γ (or equivalently the shortest Delaunay triangulation (DT) edges) are nicely correlated with λ as

$$\lambda = C\gamma^{2.5}\chi(\gamma) \text{ with } \chi(\gamma) = 1 - 0.5e^{-3\gamma}, \ C{\sim}0.2. \quad (4)$$

Astonishingly, this microstructural model, that resembles lubrication theory, is valid at high and moderate porosities for both ordered and random configurations. Henceforth, the drag force density in the fluid, $\vec{f}_i^D$ is defined at a point x_e as

$$\vec{f}_i^D = \beta\big(\langle\vec{u}\rangle - \vec{u}_i\big)\psi\big(x - x_e\big), \qquad (5)$$

where u_i is the instantaneous velocity of the ith particle and ψ is a function describing the influence of the force density in its neighborhood. While for ψ several possibilities exist, we restrict ourselves to $\psi(x\text{-}x_e) = \delta(x\text{-}x_e)$, i.e. the Dirac delta function.

In the next section the above drag force density is used to explicitly couple the fluid and particle dynamics.

MATHEMATICAL FLUID MODEL

The governing equation for the multiphase flow is a set of porosity scaled Navier-Stokes equations, which define the flow of fluid in a particulate porous media. Considering an incompressible fluid (i.e. the density, ρ is constant) in an Eulerian flow domain, Ω, we can write the equations of both fluid and solid phase as

Fluid phase:

$$\left.\begin{aligned}
&\rho\frac{\partial(\varepsilon\vec{u})}{\partial t} + \rho\nabla\cdot(\varepsilon\vec{u}\vec{u}) = -\varepsilon\nabla p + \nabla\cdot(\varepsilon\boldsymbol{\tau}) + \varepsilon\rho\vec{g} - \sum_i \vec{f}_i^D \\
&\boldsymbol{\tau} = \mu\big(\nabla\vec{u} + (\nabla\vec{u})^T\big) - \frac{2}{3}\mu(\nabla\cdot\vec{u})\mathbf{I} \\
&\frac{\partial\varepsilon}{\partial t} + \nabla\cdot(\varepsilon\vec{u}) = 0
\end{aligned}\right\} \text{ in } \Omega$$

Solid phase:

$$\left.\begin{aligned}
&m_i\frac{d\vec{u}_i}{dt} = \vec{F}_i^D + \sum_j \vec{F}_{ij}^C - V_i\nabla p + m_i\vec{g} \\
&I_i\frac{d\vec{\omega}_i}{dt} = \mathrm{T}_i^D + \sum_j r_i\hat{n}_{ij}\times\vec{F}_{ij}^C
\end{aligned}\right\}, \qquad (6)$$

where p, τ and g are pressure, shear stress and the acceleration due to gravity, respectively. For the particles m, I_i, r_i, V_i, u_i and ω_i represent particle mass, moment of inertia, radius, volume, translational and angular velocity, respectively. The $\vec{F}_{ij}^C$ represents the inter-particle/wall contact force and n_{ij} is the unit vector pointing from the center of the particle to the contact point (with particle j). A linear spring-dashpot model was used for the contact force. Finally, $\vec{f}_i^D$ and $\vec{F}_i^D$ represent the drag force per unit volume on the fluid due to interaction with the ith particle and the total drag force acting on the ith particle, defined in previous section. In the angular momentum equation, T_i^D represents the torque experienced by the ith particle due to fluid drag when flow around the particle becomes asymmetric. The pressure gradient term in Eq. (6) accounts for the net buoyancy force on each particle passing through its center. Since Eq. (6) is a system of ordinary differential equations in time, it can be integrated using a suitable numerical integrator. For accuracy and conservation properties, we use the velocity-Verlet time integrator, which is second order accurate in time.

The FE mesh adapted in the above formulation is a Delaunay triangulation (DT) based on the particle locations, which serves both as a contact detection tool

and a FEM mesh. This implies that all interior vertex nodes of the mesh are occupied by particles at all times, while the boundary nodes are inserted only for the convenience of computation and application of boundary conditions, see Fig. 1. In the following, this computational framework will be used to simulate several test cases for both static and moving particles.
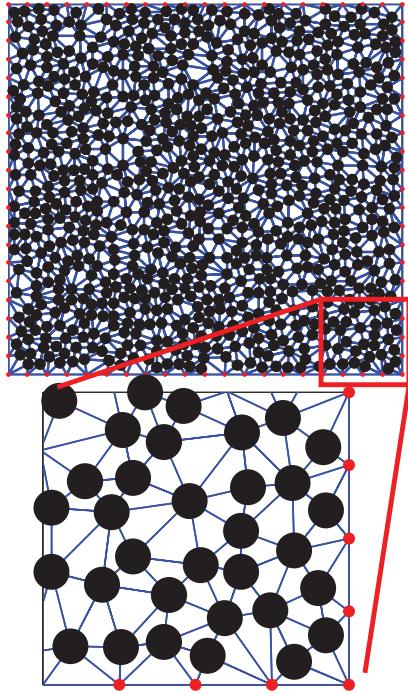

FIGURE 1. Finite element mesh based on 800 randomly distributed particles at porosity 0.6. (Top) complete mesh; (Bottom) Zoomed in, lower right corner, which shows the added boundary nodes (red points) to define the grid, distributed at equal distances of ~2d.

Static Particles

For this test case in a square domain, the top and the bottom boundaries have no-slip boundary conditions, while the left and right boundaries maintain a pressure gradient of 5 [kg/(m^{2}s^2)], see the inset of Fig 2. With decreasing porosity, the flow gradually confines itself between the walls and the top and bottom rows of particles as the interior becomes less and less permeable. For comparison purposes the average flow velocity is computed for the entire domain and compared with finely resolved FEM simulations in Fig. 2. The average flow predictions for both the ordered and random case agree well with data from finely resolved FEM simulations. The overall fit follows the finely resolved curve. Note that the fully

resolved simulations are geometrically correct, i.e. particles are represented by holes with no-slip boundary conditions and contain more than 10^5 degrees of freedom (dof). Our coupled simulation, in contrast, relies only on a few hundred dofs of the DT.
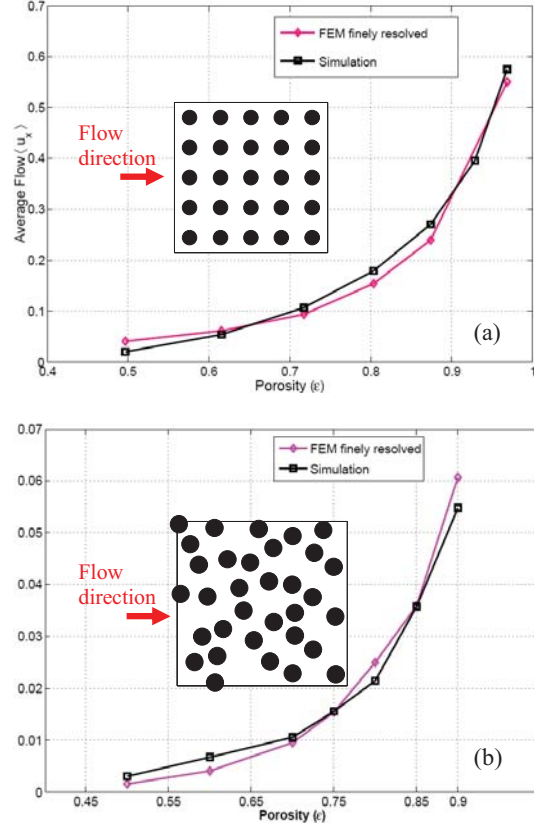

FIGURE 2. Average horizontal fluid velocity plotted against porosity through (a) ordered and (b) random fibre arrays.

Moving Particles

A particle under gravity in a viscous fluid, both initially at rest, will fall until it has reached the settling/terminal velocity, u_s calculated using the drag law prescribed in [12]. No slip boundary conditions are used at the top and bottom walls, while friction-less (no shear stress) boundary conditions are used along the left and right walls. The particle is released from $Z_0 = 0.6H$, where $H = 2$ [m] is the height of the box, see Fig. 3. The mesh is based on a single particle location (corner points and two additional boundary points on each wall) and consists of only 12 triangular elements, which is rather coarse. Here we switch to 4th order polynomials for an increased flow resolution. The settling velocity can be computed when the frictional force, f^D, combined with the buoyancy force

exactly balance the gravitational force (*mg*) and is equal to $u_s \sim 0.17$ [m/s]. Figure 3 shows the deforming mesh as the particle follows its trajectory. Near the particle surface a halo region with non-zero upwards fluid velocity appears due to the drag exerted by the falling particle. A trail of this halo is not evident since viscosity is large and our approach does not fully resolve the flow. Note that for this particular case no re-meshing was required as the mesh does not entangle or deteriorate throughout the simulation.
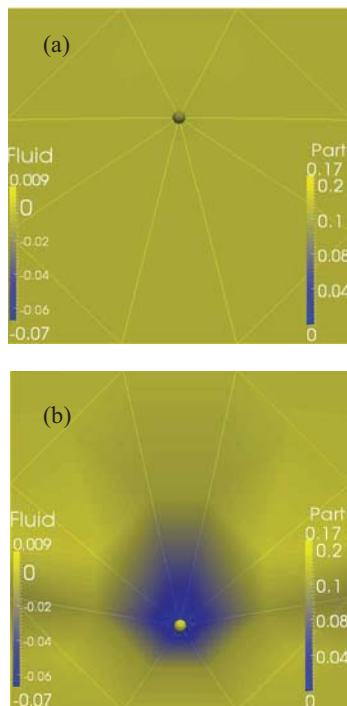

FIGURE 3. Deforming mesh with velocity contours for 1 particle settling using 4th order basis functions at (a) $t = 0.25$ [s] and (b) $t = 2$ [s]. The velocity of the falling particle quickly attains its settling velocity of $u_s \sim 0.17$ [m/s].

SUMMARY AND CONCLUSIONS

We present a monolithic method for two-way fluid-particle coupling on an unstructured mesoscopically coarse mesh. In this approach, a higher order finite element method (FEM) on a moving mesh for the fluid phase is combined with a soft sphere discrete element method (DEM) for the particles. The main feature of our approach is a deforming Delaunay triangulation based on the particle centers of mass, which is utilized as an efficient contact detection tool for the moving particles and as the FE mesh for discretizing the Navier-Stokes equations. Two-way momentum exchange is implemented using semi-empirical drag laws, for which the microstructure has a strong effect. Lubrication theory works astonishingly well, when the 2nd nearest neighbor distances (or equivalently the shortest Delaunay edges) are considered, since they represent the relevant network for the flow. We validate the methodology with several test cases, including flow through porous media, which is compared against finely resolved FEM simulations. The real two-way coupling for moving grains and adaption to more interesting/relevant situations (such as fluidized beds with heat/mass transfer) is part of an ongoing research [13]. Moreover, applying such a computational framework in more complex situations involving deformable granular solids is still a challenge for future study.

REFERENCES

1. H.P. Zhu, Z.Y. Zhou, R.Y. Yang, A.B. Yu, *Chemical Engineering Science* **63**, 5728–70 (2008).
2. K. Yazdchi, S. Srivastava, S. Luding, *Int. J. Multiphase Flow* **37**, 956-66 (2011).
3. K. Yazdchi, S. Srivastava and S. Luding, *Composites Part A* **43**, 2007-2020 (2012).
4. K. Yazdchi, "Micro-macro relations for flow through fibrous media", Ph.D. Thesis, University of Twente, 2012.
5. W.J.B. Grouve, R. Akkerman, R. Loendersloot, S. van den Berg, *Int. J Mater Form,* Suppl **1**, 859–862 (2008).
6. S. Luding, *Granular Matter* **10**, 235-246 (2008).
7. N. G. Deen, M. A. van der Hoef, M. V. Annaland, and J. A. M. Kuipers, *Progress in Computational Fluid Dynamics* **7**, 152–162 (2007).
8. J.M. Rotter, F.G. Holst, J.Y. Ooi, and A.M. Sanad, *Phil. Trans. R. Soc. Lond. A* **356**, 2685–12 (1998).
9. P.A. Vermeer, S. Diebels, W. Ehlers, H.J. Herrmann, S. Luding, and E. Ramm, Berlin, *Lecture Notes in Physics* **568**, (2001).
10. J. Gan, H. Zhao, A. S. Berrouk, C. Yang, H. Shan, *Powder Technology* **218**, 69–75 (2012).
11. K. Yazdchi and S. Luding, *Chemical Engineering Journal* **207**, 35-48 (2012).
12. A.P. Peskin, G.R. Hardin, *J. Research of National Inst. Standards and Technology* **103**, 77-91 (1998).
13. S. Srivastava, K. Yazdchi, S. Luding, in preparation.